Automatic Segmentation Measuring Function for Cardiac MR-Left Ventricle (LV) Images

D.N.F. Awang Iskandar, A. Khan, P.C. Lim and Y.C. Wang
Faculty of Computer Science and Information Technology,
Universiti Malaysia Sarawak, 94300 Kota Samarahan, Sarawak, Malaysia.
dnfaiz@unimas.my

Abstract—**Automatic segmentation approaches are a desirable solution for Endocardium (inner) and Epicardium (outer) contours delineation using cardiac magnetic resonance left ventricle (CMR-LV) short axis images. The Level Set Model (LSM) and Variational LSM (VLSM) is the state-of-the-art in detecting the inner and outer contour for medical images. However, in CMR-LV images segmentation the LSM and VLSM are facing with the issue of re-initialisation because of irregular circle shape. In this paper, we developed an automatic segmentation measuring function based on statistical formulation to solve the re-initialisation issues in huge set of data images. The sign Euclidean distance function successfully classified the negative (inner contour) and positive (outer contour) features. The Fuzzy C mean interaction operator intersects the high membership degree that initialises the centre point. The experiments were conducted using the Sunnybrook and Pusat Juntung Hospital Umum Sarawak (PJHUS) cardiac datasets. This paper aims at developing a distance function to guide the automatic segmentation for LV contours and also to reduce segmentation error.**

Index Terms—**VLSM; Sign Euclidean Distance Function; Fuzzy C Mean Interaction Operator; Segmentation Error.**

I. INTRODUCTION

Cardiac magnetic resonance (CMR) is one of the most usable diagnostic technologies that observe the behaviour of the human heart. This technology generates the morphology of the right ventricle (RV) and left ventricle (LV) and also explores cardiac parameter for the estimation of cardiac function. It is frequently applied for the diagnosis and acute examination of cardiac abnormalities. Segmentation methods are categorized into three main approaches – manual, semi-automatic and fully automatic approach. The manual segmentation approach is known to be prone to error, tedious and requires human expert for LV contours tracing in huge number of images [1]. The semi-automatic segmentation approach improved the manual segmentation approach and introduced the systematic solution in clinical observation [2]. Recently, the guide point model approach by the use of radial snake model approach is adopted and developed into a semi-automatic commercial application for LV contours segmentation [3]. Lastly, the fully automatic segmentation approach fulfils the requirement of both existing approaches and introduced different type of segmentation techniques in different style. The researchers and computer scientist still focus on developing a competent automatic method, that's why the cardiac LV is an open research area for cardiac researchers. A few related techniques, including shape detection method [4], seed point classifier (region growth) [5], diffusion-based unsupervised clustering technique by image-driven approaches [6], GVF snake algorithm [7] and geometric LSM approach [8].

In medical terminology, the CMR-LV contours are very important for automatic segmentation as myocardial infraction (MI) normally affects the LV. The oedema and cell injury are normally occurring in the myocardial muscle. The LV is comprised in three layers that are Endicardium (outer) layer, Myocardium (middle) and Epicardium (inner) layer [9]. In clinical routine experience, the outer layer is thin and connected with fat and other tissue which serve as protection and allows the pumping of blood. The middle layer is situated between outer and inner layer that connect the myocardial muscles known as cardiomyocyte. The muscles assist the connection between outer and inner layers during relaxation time. Finally, the inner layer is a proactive and smooth layer that connected with inner appendages and allows the steady flow of the blood.

This research focuses on developing the automatic segmentation measurement function to automatically calculating the distance between inner and outer contours. The developed function follows the sign Euclidean function formulation to map the distance of slice-by-slice of CMR-LV of each patient. The developed segmentation algorithm allows automatically segmentation of the LV contours with the aim to solve the re-initialisation issue and reduces segmentation error. Besides being a part of a quantitative research, the function requires statistical and mathematical formulation which makes it possible for the prediction of cardiac diseases.

The objective of this paper is to present an automatic segmentation measuring function by integrated sign Euclidean distance function. The developed distance function measures the distance from (i) the identified centre location of LV to the inner contour; (ii) from the inner contour to outer contour in a set of slices of per patient CMRI. In the pre-processing stage, morphological and Otsu threshold method which remove the unwanted papillary muscles and heterogeneity in image pixels [10] and [11] is integrated. The Fuzzy C mean intersection operator to identify the centre point [12] provides the starting point before calculating the distance of the inner contours. Finally, the developed distance measuring function is used to reduce the segmentation error in CMR-LV short axis images.

II. BACKGROUND STUDY

From last two decades, segmentation approaches have played a major role in diagnosing the cardiac abnormality. There are various studies that described the segmentation curves evolution for medical images. Fronts propagating with

curvature-dependent speed model by using the Hamilton-Jacobi formulations and propagating speed curvature (PSC) algorithm is introduced in [13]. The model imitates the statistical formulation based on right hand rule. The model automatically segmented the surface area of the moving circle shape images. The motion surface by curves evaluation method is shown in the following formula:

$$x_t = f(k) . \frac{y_s}{(x_s{}^2 - y_s{}^2)^{1/2}} \qquad (1)$$

$$y_t = f(k) . \frac{x_s}{(x_s{}^2 - y_s{}^2)^{1/2}} \qquad (2)$$

where f represent the speed function of k curvature. The $x(s,t)$, $y(s,t)$ represent the position vector and s denoted the parameterised function of axis t. Therefore, the $f(k)$ function processes the s parameters of k curvature to iterate the internal shape features. $k = \frac{y_{ss} x_{s-} x_{ss} y_s}{(x_s{}^2 + y_s{}^2)}$ represents the generated map of k curves of a given circle.

Later, a model that integrates [13] and the Piece Wise Smooth function (PWS) with some additional changes was introduced in [14]. This model presented the weak points of variation problem in eye retina images. The algorithm was tested on the physical structure of eye retina images used optimal function to measure the distance between retina and light. The model [14] developed an equation for inside and outside circle detection as defined below:

$$\begin{aligned} f_1(c) + f_2(c) = &\int_{inside} |u_0(x,y) - c_1|^2 \, dx \, dy \\ &\ldots\ldots + \int_{outside} |u_0(x,y) - c_2|^2 \, dx \, dy \end{aligned} \qquad (3)$$

where f indicate the energy function of curvature line, the c_{inside} and $c_{outside}$ indicate the contours position. The model explained that u_0 define the input image, if the $u_0 \approx u_o^i$ indicated the inside objects and $u_0 \approx u_o^0$ represent the detected outside objects. The resulted images produced the local minimum objects boundaries, meanwhile the regularisation function solved the issue of global minimiser, which act on all curves and produced the global minimiser.

Recently, the LSM and VLSM approaches were commonly used for CMR-LV contours segmentation. Both approaches generate the curvature lines for segmenting the inner and outer contours of LV. The LSM approach contributed the fast distance preserving level set evolution approach [15] which detects the negative and positive feature concept for curvature evolution. The approach calculates the numbers of iteration in minimum time. The approach also describes the speed function that forces the curvature toward the circle shape boundary. Equation of fast distance preserving level set evolution approach is defined below:

$$\frac{\partial \emptyset}{\partial t} + F|\nabla \emptyset| = 0 \qquad (4)$$

where F define the speed function, which load the patient data and $\emptyset$ is the level set function. To avoid the LSM re-initialisation issue, the sign distance function act as a numerical and particle remedy in traditional methods as:

$$\frac{\partial \emptyset}{\partial t} = sign(\emptyset_0)(1 - |\nabla \emptyset|) \qquad (5)$$

where $\emptyset_0$ define the re-initialised function and $\emptyset$ is the LSM sign distance function. In this case, if the circle surface area is smooth then the curves line process well otherwise chances of conflict. To avoid this issue, the new VLSM with penalising energy approximate the $\emptyset$ function. Equation below defines the formula for penalising energy:

$$p(\varphi) = \int_\Omega \frac{1}{2} (|\nabla \emptyset| - 1)^2 \qquad (6)$$

where p is the penalizing energy that drive the motion of the $\emptyset$ towards in to Ω image domain. During the $\emptyset$ implementation the curves evaluation degraded due to some extent or location, the issue had solved by distance regularized level set evolution [16], which followed the energy formulation with distance regularisation function if $\Omega \rightarrow R$ then the energy function $\in (\emptyset)$. This study [16] has become popular because of statistical evaluation techniques. There are various formulas introduced on the base of existing literature, some common equations used in medical images segmentation are show in below:

$$\in (\emptyset) = uR_p (\emptyset) + \in_{ext} (\emptyset) \qquad (7)$$

where R_p represent regularisation function with $\emptyset$, $\in_{ext}$ represent the energy forced for internal circle detection. Then the energy function forced for external shape feature detection, thus the $R_p (\emptyset)$ is:

$$R_p (\emptyset) \underline{\triangleq} \int_\Omega p (|\nabla \emptyset|) \, dx \qquad (8)$$

where p define the potential energy $p : (0, \propto) \rightarrow R$ that forced the internal energy toward objects boundary. Equation (8) has integrated Variational level set fitting technique [17] which detected the objects in computed tomography images. Equation (9) below show the fitting technique formulation at level set $\emptyset$ curves evolution:

$$E(\emptyset) = up((\emptyset) + E_G , Λ, \propto (\emptyset) \qquad (9)$$

where E_G define external energy and the $Λ$ derive zero $\emptyset$ towards objects boundary. This technique has become popular in other medical images including X-ray and computed tomography (CT) images or any other noisy medical images. The Variational level set fitting technique [17] is prone to error when the images topology changes. To avoid this issue, the fitting technique follows the penalize energy as below:

$$\begin{aligned} \frac{\partial E}{\partial \emptyset} = &-u \, [\, \Delta \emptyset - div(|\nabla \emptyset|)] - \\ &Λ\delta (\emptyset). div (\delta) - \\ &\ldots\ldots \infty \in (\emptyset) \end{aligned} \qquad (10)$$

The Variational model takes the coefficient of the negative values, to speed up the $\emptyset$ function. The equation had been tested on different types of medical images domain and conducted competitive results at different studies with different style [18].

III. PROBLEM FORMULATION

Automatic segmentation of CMR-LV contours for a series of slices of per patient is a challenging task. The LSM and VLSM approaches face the issues of irregular shape identification and re-initialisation because of unstructured shape CMR-LV images. Another reason is the huge set of short axis slices per patient. To overcome this issue, an automatic segmentation measuring function is develop to reduce the contours segmentation error in CMR-LV short axis images and hopefully to find good used in other medical images.

IV. METHODOLOGY

The manual segmentation approach is tedious, time consuming and seldom leads to error in processing huge amount of CMR-LV short axis images. To overcome this issue, different automatic segmentation methods were developed but still there is the need of a competitive method in CMR-LV slice-by-slice segmentation. In this paper, first we explain the methodology of the developed automatic segmentation measuring function approach, which combine the sign Euclidean distance function to classify the negative (inner) and positive (outer) features in CMR-LV context and measures the distance among inner and outer contours. The approach has a great interest to solve the irregular shape and re-initialisation issues that can only possible by the use of statistical formulation. The proposed methodology for the automatic segmentation measuring function is described in following sections.

A. Automatic LV Localisation
Equation (11) indicate that a specified heuristic threshold value, which set by default to find out the beating heart area during a cardiac cycle.

$$Cimg(i,j) = \begin{cases} start\ 0, & if\ simg(i,j) => T \\ Next & Then\ load next\ slice \end{cases} \quad (11)$$

where T indicates the heuristic threshold value that represents the process of default threshold value between the ranges of 0 up to 170. $Simg$ represents the starting slice where the algorithm takes the initial slice from given patient data file/directory. The i,j represent the processing per slice pixels position. The heuristic threshold value automatically changes with changing the number of slices. The equation guide the suggested algorithm to continuously process the slices of per patient until the end slice and finally the features of LV area are identified. In this process, the algorithm need to firstly understand the behaviour of CMR-LV short axis images where all the slices of per patient data file were collected from movies (scan type). As there are a series of between 240 to 250 slices per patient, it is quite difficult to classify the shape features slice-by-slice. A predefine threshold value is set that automatically change the position of the given slice to identified the good feature of beating area, which includes the LV area. This is achieved using an integrated time based and shape based approach [19].

B. Papillary Muscles Removal
The morphological operation, anisotropic diffusion functions and Otsu threshold are the integrated methods from existing studies [10], [11] and [12]. These techniques are used to remove the papillary muscles before initiating the automatic segmentation. The morphological disk operation with disk size 3 is applied on starting slice to obtain the structure element $g(x)$, then the dilation of g by x are express in below equation (12):

$$g(x) = Simg(y \in f)[g(y) + Simg(x - y) \quad (12)$$

where f represent the calculated area of mid cavity, y represent the variable used for the removal of papillary muscles location. But because of detecting the extra region of inner contour during the experiments we notice that the dilation operation lead to some changes in cavity size and thus the actual size is missed. To solve this issue, we used erosion operation which removes the extra regions and give the output as actual size.

C. Centre Point Identification
The Fuzzy C Mean intersection operator intersects the high membership degree to identify the centre location of set of slices. In equation (13), let i, j represent the pixels' values and z represent the universe point, then

$$\mu_{i \cap j}(z) = \min\{ \mu_i\ (z), \mu_j(z)\} \quad (13)$$

where i, j represent the pixels' values and z represent the universe point, μ indicate the parameter functions, which taking the mean value of high membership degree of each slice-by-slice of per patient. The intersection operator used the pixels i, j values and gives the high membership degree value, which is the z universe point. The below equation (15) show that:

$$z = (i - j): i \in I, j \in T \quad (14)$$

If $i - j = 0$ indicates no difference and $i - j \neq 0$ indicates difference in pixels. Then the $z > i - j = 1$, that is presenting the high membership degree in a single slice. This universe point is actually the high membership degree, which means the centre point of CMR-LV localised images.

D. Automatic Segmentation Measuring Function
In slice-by-slice automatic segmentation, it is very difficult to segment all the slices at once. The proposed distance function method combines the sign distance and Euclidean distance functions to solve this traditional well known segmentation problem in CMR-LV images. First, we measured the distance of inner contour from identified centre location using the sign distance function. The equation starts from identified centre location and guide the algorithm on right hand rule to draw the boundaries mask following by negative shape feature information using the localised shape pixels. Equation (16) is defined for initialisation of inner contour:

$$C(c_{inner}, c_{outer}) = \int_{\Omega}(|\nabla \emptyset| + l_{min})dx \quad (15)$$

where $C(c_{inner}, c_{outer})$ defines the segmented Endocardium (inner) and Epicardium (outer) contours, $\emptyset$ represent the sign distance function, Ω is the level set cures, $\int_\Omega$ define a delta function to speed up the level set cures. In order to avoid the re-initialisation and variational issue as in level set cures evaluation, equation below is used to fix the distance map followed by centre location:

$$C(c_{inner}) = \{z_\mu \in \Omega | \emptyset\left(z_\mu\right) = 1 \qquad (16)$$

where z_μ denote the mean of centre location, which initialise the distance line up to inner contour in set of slices. Thus, the combine sign Euclidean distance function taking the distance measurement, from centre to Endocardium contour towards Epicardium contour. But due to the variation issue in the shape features we integrated the approach done in an existing study [16], which assume that $\emptyset$ is parameterised not only by z_μ but also required a standard time t. Thus, the distance mapping technique guide the curves in specified t toward the decent direction follows an energy function e_f, that is:

$$e_f = \mu P(\emptyset) + d_m(\emptyset) \qquad (17)$$

where μP represent the mean of distance parameters and $d_m(\emptyset)$ define the distance moving function, which move distance parameter towards c_{inner}, c_{outer} contours. This distance function initially solved the re-initialisation issue by $\emptyset$ function and the e_f force the energy function, which followed the measured distance function. Finally, our proposed distance function followed the penalize energy function and delta function to measure the both contour and make it ready before automatic segmentation algorithm process.

E. Segmentation Error

To calculate the error between manual and automatic drawn contours, the statistical method standard error (SE) estimate the sample mean of measured area from the population of sample slices, which is explain in equation (18):

$$SE_{\mu_{sample}} = \frac{std}{\sqrt{n}} \qquad (18)$$

where $SE_{\mu_{sample}}$ define the standard error in given slices data. std represents the standard division, which estimate the difference between manual and automatic value. The $\sqrt{n}$ defines the sample mean of both manual and automatic segmented contours. Equation (18) estimates the sample mean of segmented contours from the population of sample slices and give the error in manual and automatic segmentation.

V. EXPERIMENTAL DESIGN

Before being able to detect the LV contour automatically, the identification and measurement of inner and outer contours are the primary task to be completed. The experiments were conducted to analyse the effectiveness of the developed automatic segmentation measuring function.

The sign Euclidean distance function measure the contours distance based on negative (inner) contours features and positive (outer) contours features. The automatic segmentation algorithm uses the measured distance map and segments the inner and outer CMR-LV contours. The segmented result images aim to show the measured size of the inner and outer contour. The function process slice-by-slice CMR-LV images of a patient and is tested on all patient data from the two datasets.

A. Dataset Collection

The experiments were carried out on two cardiac data sets. Data in both cardiac datasets are collected after heart attack – infraction or myocardia infraction between the slice number 240 and 250 of a patient. Brief summary on both datasets is described in following paragraph.

The first dataset is the Sunnybrook cardiac data (SCD) published by the Health Sciences Centre Toronto hospital [20] held by MICCAI workshop in 2009. The SCD dataset contain 45 patients which includes heart failure with infarction (HF-I) with late gadolinium (Gd) enhancement, heart failure without infarction (HF-NI) with no late Gd enhancement, LV hypertrophy (HYP) with LV mass and surface area and Healthy present by (N) with no hypertrophy. The data are categorized into training dataset which consist of 12 patients of HF-I, HF-NI, HYP and N, testing dataset (12 patients), validation dataset (12 patients) and normal dataset (9 patients). The manually traced contours are used as ground truth in segmentation experiments.

The second dataset is the PJHUS cardiac dataset where all the patient data were collected from local Sarawak General Hospital Heart Centre by cardiac expert. The dataset was collected on 10 patients of different ages and gender.

B. Image Analysis

The total number of slices is in each data sets are 240, all the slices are presented in DICOM formatted. The size of pixel of each slice is 110*110. Field of view (fov) is 320 mm*320mm, thickness of 8-10mm, slice gap of 0mm and resolution of 0.2.

C. Experiment Platform

The experiments were conducted on Dell system with Intel® Core™ i5-6200 CPU, 2.40 GHz along with 8.00 GB memory and 64-bit processing time. MATLAB 2015 was used for statistical calculation. The R language and C programming languages are used.

VI. RESULTS & DISCUSSION

Searching of objects by the way of automatic technique is much difficult and faster as compared to manual method. The existing segmentation approaches tracing LV contours by selecting manually the given image position, which had considered semi-automatic. In CMR-LV images, we have segmenting the LV contours by automatic solution. In implementation, we notice the issues of contours boundary specification and in large set of data we loss the accuracy. To reduce the segmentation error in 240 slices of each patient file, this section discusses the develop distance measurement function in estimating the distance between inner and outer contours.

In Figure 1, samples of localised slice taken from both SCD and PJHUS cardiac data are shown where the unwanted

papillary muscles were removed by morphological operation (discussed in Section IV, A). Without removal, these muscles cause issue to inner contour measuring, which later led to issue in re-initialisation. Also, the ROI mask presents the localised are of LV.
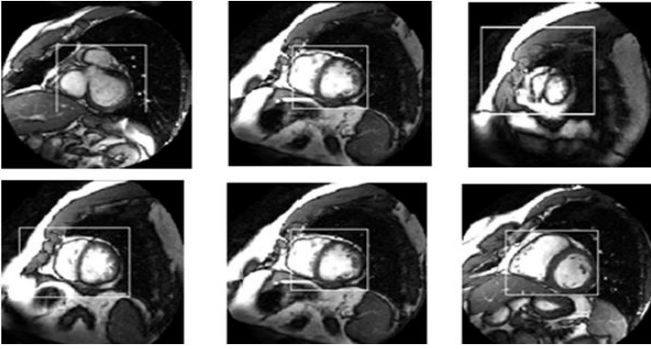

Figure 1: Snapshots sample of localised LV

Figure 2 showed the experimental result images by the used of equation (14) and (15). Only when the membership degree is 1, the algorithm continues with the process and successfully detected the centre point (indicated by "+"). This centre point is the initialise location for measuring function to start the estimation of negative and positive features, while the segmentation algorithm used this centre point to measure the distance of inner and outer contour.
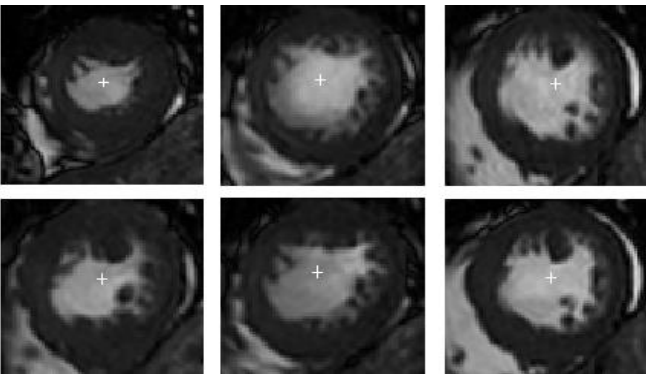

Figure 2: Samples of automatic identified centre location of LVs

The ground truth resulted contours values of Sunnybrook and PJHUS cardiac data are expressed in percentage. This value shows the average percentage of manual detected inner and outer contours. The experimental work show the performance of the developed function tested on Sunnybrook and PJHUS cardiac datasets with encouraging results. The Figure 3 and Figure 4 present the measuring function, the blue lining represent the distance map for inner and outer contours. The green circle represents the outer contour map and the red circle represents the inner contour map.

In Figure 3, result images of measuring function by follows the equation (16) are shown where the distance is represented by colour lines. The sign distance function (negative features) measurement towards inner contours from centre point is represented as dark-red colour. The * represents the convolution operator, which points out the desired area for the segmentation algorithm. The blue line show the measured distance based on equation (17). The blue line represents the (positive features) mean outer contours. Finally, the dark-green lining represents target position of outer contours that reduces the segmentation error.
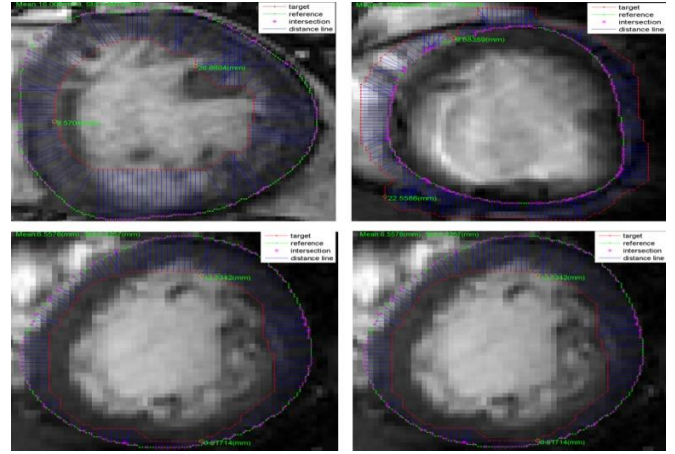

Figure 3: Snapshot sample, the red show inner contour, blue is the distance line and green outer contour (best viewed in colour).
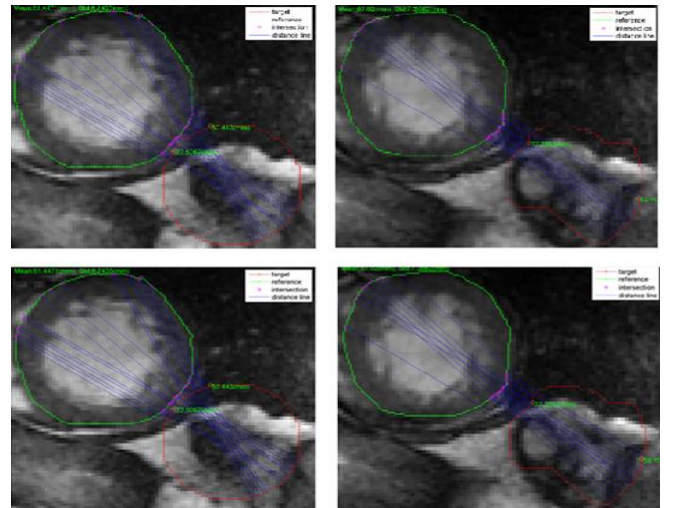

Figure 4: The sample show the distance in separated views (best viewed in colour).

Figure 4 showed the measured function at separate view where the dark red represent the measured area of inner contour, the blue lines represent the measured area of outer contours and the dark-green define the target location.

The comparison between the segmented contours values of SCD cardiac HF-I dataset is reported in Table 1. The First column shows the ground truth value of segmented outer and inner contours. The second column shows the proposed segmented contours values that we almost published in our previous work [19]. The comparison among ground truth and proposed segmented values describing the accuracy based on experimental output images in Figure 5 where the highlighted contours are in blue. The red colour represents the inner contour which shows the missing contour. The blue colour presents the segmented contours in each slice.

The third column in Table 1 shows the resulted values of segmentation error through segmentation error formulation (18). The error is describing the distance among inner and outer contours. The bold values represent the high accuracy in segmented contours. The segmentation approach still needs to improve for other segmented values, which we show in our future work. The results were conducted based on measuring function, the results are very encouraging as compare with ground truth values.

In Table 2 we present the comparison between segmented contours of PJHUS cardiac dataset. The dataset consists of 10

patients, all the data file arranged after the MI. The Syngo online software [21] process the 10-patient data and view the per patient data file. The software highlighted the inner and outer contours area in slice-by-slice view and we first manually segmented the inner contour and then manually segmented the outer contours. The process is repeated for the 10 patients. After a successful manual correction in LV contours, we conducted the manual segmented contours values reported in Table 2. The proposed values come after the evolution of automatic segmentation measuring function. The proposed results are very encouraging as compare with manual segmentation results. Beside the segmentation error describe the difference between manual and automatic contours segmentation values.

The segmentation error determines the difference among manual and proposed results. The difference present that our proposed method reduces the segmentation error based on measuring function. The function calculates the distance in each slice contour and sequentially process the per patient data file. The calculated distance creates a map of inner and outer contour. The automatic segmentation approach follows the map and segmenting the inner and outer contour of per patient set of slices. The function also solves the re-initialisation issue based on distance mapping method. Now the segmentation method only segmented the identified objects of inner and outer contours. Although the proposed method introduces very encouraging solution, that solved the re-initialisation problem and reduces the segmentation error and the function are very productive for future research.

Table 1
Ground truth value of segmented contours, prosed segmented contours values and segmentation error

| Patient _id | Sunnybrook cardiac dataset | | | | | |
| | Ground-truth | | Proposed | | Segmentation error | |
	Outer	Inner	Outer	Inner	Outer	Inner
SC-HF-I-1	75.5	100	**94.5**	**100**	9.53	0.00
SC-HF-I-2	88.4	100	**89.5**	**100**	0.57	0.00
SC-HF-I-4	79.3	90.2	86.3	100	3.51	0.00
SC-HF-I-05	70.5	90.3	**100**	**100**	14.74	4.84
SC-HF-I-06	86.3	100	**96.2**	**100**	4.83	0.00
SC-HF-I-07	84.0	95.0	88.3	100	2.17	2.49
SC-HF-I-08	80.5	92. 2	84.6	100	2.07	3.89
SC-HF-I-09	76.8	86.8	80.5	92	1.58	2.57
SC-HF-I-10	82.3	92.3	85.4	100	1.57	3.84
SC-HF-I-11	87.6	100	93.0	100	2.69	0.00
SC-HF-I-12	92.7	100	94.0	100	0.64	0.00
SC-HF-I-40	92.3	100	**95.3**	**100**	1.50	0.00

Table 2
Syngo online software value of segmented contours, proposed segmented contours values and segmentation error.

| Patient _id | PJHUS cardiac dataset | | | | | |
| | Synago online software [21] | | Proposed | | Segmentation error | |
	Outer	Inner	Outer	Inner	Outer	Inner
Patient 001	**83.2**	**96.3**	**97.5**	**100**	7.18	3.34
Patient 002	**87.6**	**97.0**	**92.2**	**100**	2.32	1.04
Patient 003	82.0	96.8	89.4	100	3.72	1.59
Patient 004	82.5	98.0	99.3	100	8.04	0.99
Patient 005	85.0	97.7	94.6	100	4.83	1.14
Patient 006	87.0	98.4	93.3	100	3.18	0.79
Patient 007	86.2	95.9	89.4	100	1.62	2.04
Patient 008	87.0	94.8	90.6	100	1.80	2.59
Patient 009	80.3	95.2	83.1	100	1.42	2.39
Patient 010	87.9	98.5	90.2	100	1.16	0.74
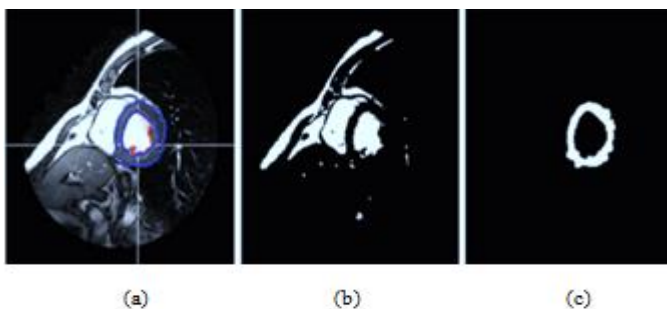
Figure 5: (a) automatic contours segmentation, (b) edge base method and (c) muscles (best viewed in colour).

VII. CONCLUSION

In this paper, we present the development of an automatic segmentation measuring function that measures the distance between two contours in CMR-LV. The integrated sign Euclidean distance function classify the negative and positive features of contours. The developed function follows the features and draws a distance line which further guide the automatic segmentation method to segment the actual size of inner and outer contours. This method is developed for a fully automatic segmentation of CMR-LV short axis slice-by-slice contours measuring to identify the actual size of inner and outer contours and it is proven to reduce the error in contours segmentation. Our future works include automatic segmentation of Endocardium and Epicardium contours, which will generate the automatic assessment solution for cardiac function.

REFERENCES

[1] Üzümcü, M., van der Geest, R. J., Swingen, C., Reiber, J. H., & Lelieveldt, B. P. (2006). Time continuous tracking and segmentation of cardiovascular magnetic resonance images using multidimensional dynamic programming. *Investigative radiology*, *41*(1), pp. 52-62.

[2] Auger, D. A., Zhong, X., Epstein, F. H., Meintjes, E. M., & Spottiswoode, B. S. (2014). Semi-automated left ventricular segmentation based on a guide point model approach for 3D cine DENSE cardiovascular magnetic resonance. *Journal of Cardiovascular Magnetic Resonance*, *16*:8.

[3] Bessa, J. A., Cortez, P. C., da Silva Félix, J. H., da Rocha Neto, A. R., & de Alexandria, A. R. (2015). Radial snakes: comparison of segmentation methods in synthetic noisy images. *Expert Systems with Applications*, *42*(6), pp. 3079-3088.

[4] Gering, D. T. (2003, November). Automatic segmentation of cardiac MRI. In *International Conference on Medical Image Computing and Computer-Assisted Intervention*. Springer Berlin Heidelberg, pp. 524-532.

[5] Kaus, M. R., von Berg, J., Weese, J., Niessen, W., & Pekar, V. (2004). Automated segmentation of the left ventricle in cardiac MRI. *Medical image analysis*, *8*(3), pp.245-254.

[6] El Berbari, R., Bloch, I., Redheuil, A., Angelini, E., Mousseaux, E., Frouin, F., & Herment, A. (2007). An automated myocardial segmentation in cardiac MRI. *IEEE Engineering in Medicine and Biology Society*, pp. 4508-4511.

[7] Liu, Y., Li, C., Guo, S., Song, Y., & Zhao, Y. (2014). A novel level set method for segmentation of left and right ventricles from cardiac MR images. *IEEE Engineering in Medicine and Biology Society*, pp.4719-4722.

[8] Chen, S. Y., & Guan, Q. (2011). Parametric shape representation by a deformable NURBS model for cardiac functional measurements. *IEEE Transactions on Biomedical Engineering*, *58*(3), pp. 480-487.

[9] Perry, R. (2009). Cardiac MR Left Ventricle Segmentation Challenge. *World Wide Web, http://smial. sri. utoronto. ca/LV Challenge/Home. html*.

[10] Ji, D., Yao, Y., Yang, Q., & Chen, X. (2016). MR Image Segmentation Using Graph Cuts Based Geodesic Active Contours. *International Journal of Hybrid Information Technology*, *9*(1), pp. 91-100.

[11] Gao, H., Kadir, K., Payne, A. R., Soraghan, J., & Berry, C. (2013). Highly automatic quantification of myocardial oedema in patients with acute myocardial infarction using bright blood T2-weighted CMR. *Journal of Cardiovascular Magnetic Resonance*, *15*- 28.

[12] Kadir, K., Gao, H., Payne, A., Soraghan, J., & Berry, C. (2011). Variational level set method with shape constraint and application to oedema cardiac magnetic resonance image. *17th International Conference. Digital Signal Processing (DSP)*, pp. 1-5.

[13] Osher, S., & Sethian, J. A. (1988). Fronts propagating with curvature-dependent speed: algorithms based on Hamilton-Jacobi formulations. *Journal of computational physics*, *79*(1), pp. 12-49.

[14] Mumford, D., & Shah, J. (1989). Optimal approximations by piecewise smooth functions and associated variational problems. *Communications on pure and applied mathematics*, *42*(5), pp.577-685.

[15] Li, C., Xu, C., Konwar, K. M., & Fox, M. D. (2006). Fast distance preserving level set evolution for medical image segmentation. *9thIEEE International Conference, In Control Automation, Robotics and Vision*, pp. 1-7

[16] Li, C., Xu, C., Gui, C., & Fox, M. D. (2010). Distance regularized level set evolution and its application to image segmentation. *IEEE transactions on image processing*, *19*(12), pp. 3243-3254.

[17] Gupta, S., & Kumar, S. (2012). Variational level set formulation and filtering techniques on ct images. *International Journal of Engineering Science and Technology (IJEST)*, *4*(07), pp. 3509-3513.

[18] Chan, T. F., & Vese, L. A. (2001). Active contours without edges. *IEEE Transactions on image processing*, *10*(2), pp. 266-277.

[19] Khan, A., Iskandar, D. A., Ujir, H., & Chai, W. Y. (2017). Automatic Segmentation of CMRIs for LV Contour Detection. *9th International Conference on Robotic, Vision, Signal Processing and Power Applications*. Springer Singapore, pp. 313-319.

[20] R P. Radau, Y. Lu, K. Connelly, G. Paul, A. J. Dick, and G. A. Wright. (2009). Evaluation framework for algorithms segmenting short axis cardiac MRI. MIDAS Cardiac MR Left Ventricle Segmentation Challenge, [Online]. Available: http://hdl.handle.net/10380/3070.

[21] Liao, W., Deserno, T. M., & Spitzer, K. (2008, March). Evaluation of free non-diagnostic DICOM software tools. In *Medical Imaging* (pp. 691903-691903). International Society for Optics and Photonics.